The Cryosphere, 11, 483–496, 2017
www.the-cryosphere.net/11/483/2017/
doi:10.5194/tc-11-483-2017
© Author(s) 2017. CC Attribution 3.0 License.

The Cryosphere
Open Access

Active-layer thickness estimation from X-band SAR backscatter intensity

Barbara Widhalm[1], **Annett Bartsch**[1,2], **Marina Leibman**[3,4], **and Artem Khomutov**[3,4]

[1]Zentralanstalt für Meteorologie und Geodynamik, Division Data, Methods and Modelling, 1190 Vienna, Austria
[2]Vienna University of Technology, Department of Geodesy and Geoinformation, 1040 Vienna, Austria
[3]Earth Cryosphere Institute, Russian Academy of Sciences, Siberian Branch, Tyumen 625000, Russia
[4]Tyumen State University, Department of Cryosophy, Tyumen 625006, Russia

Correspondence to: Barbara Widhalm (barbara.widhalm@zamg.ac.at)

Received: 14 July 2016 – Discussion started: 31 August 2016
Revised: 26 November 2016 – Accepted: 12 January 2017 – Published: 10 February 2017

Abstract. The active layer above the permafrost, which seasonally thaws during summer, is an important parameter for monitoring the state of permafrost. Its thickness is typically measured locally, but a range of methods which utilize information from satellite data exist. Mostly, the normalized difference vegetation index (NDVI) obtained from optical satellite data is used as a proxy. The applicability has been demonstrated mostly for shallow depths of active-layer thickness (ALT) below approximately 70 cm. Some permafrost areas including central Yamal are, however, characterized by larger ALT. Surface properties including vegetation structure are also represented by microwave backscatter intensity. So far, the potential of such data for estimating ALT has not been explored. We therefore investigated the relationship between ALT and X-band synthetic aperture radar (SAR) backscatter of TerraSAR-X (averages for 10 × 10 m window) in order to examine the possibility of delineating ALT with continuous and larger spatial coverage in this area and compare it to the already-established method of using NDVI from Landsat (30 m). Our results show that the mutual dependency of ALT and TerraSAR-X backscatter on land cover types suggests a connection of both parameters. A range of 5 dB can be observed for an ALT range of 100 cm (40–140 cm), and an R^2 of 0.66 has been determined over the calibration sites. An increase of ALT with increasing backscatter can be determined. The root mean square error (RMSE) over a comparably heterogeneous validation site with maximum ALT of > 150 cm is 20 cm. Deviations are larger for measurement locations with mixed vegetation types (especially partial coverage by cryptogam crust) with respect to the spatial resolution of the satellite data.

1 Introduction

Permafrost is defined as soil or rock that remains at or below 0 °C for two or more consecutive years (Harris et al., 1988) and currently underlies some 25 % of the Earth's land surface (Huggett, 2007). Due to global warming extensive areas where permafrost is presently within a degree or two below the melting point could be destabilized (Smith, 1990). At the global scale, increased ground temperatures could facilitate further climatic changes by releasing greenhouse gases that are currently sequestered in the upper layer of permafrost by increasing the annual thaw depth (Kane et al., 1991; Gomersall and Hinkel, 2001; Shiklomanov and Nelson, 1999; Schaefer et al., 2011; Schuur et al., 2015). The top layer of ground subject to annual thawing and freezing in areas underlain by permafrost is defined as the active layer (Permafrost Subcommittee, 1988). In this layer most ecological, hydrological and biochemical activities take place (Kane et al., 1991; Brown et al., 2000). Furthermore it is an essential climate variable for monitoring permafrost regions (Schaefer et al., 2015), making it an important factor not only at the regional but also at the the global scale. The active-layer thickness (ALT) is predominately controlled by ambient temperature but is also influenced by insulation layers such as snow cover and vegetation, slope, drainage, soil type, organic layer thickness and water content (Leibman, 1998;

Published by Copernicus Publications on behalf of the European Geosciences Union.

Shiklomanov and Nelson, 1999; Hinkel and Nelson, 2003; Kelley et al., 2004; Melnikov et al., 2004; Vasiliev et al., 2008). Due to the interaction between these surface and subsurface factors that can be spatially highly variable, ALT may vary substantially over short lateral distances (Shiklomanov and Nelson, 1999; Leibman et al., 2012).

Near-surface permafrost area is projected to decrease within the next century (IPCC, 2013). Changes in active-layer thickness have been already observed for Yamal (Leibman et al., 2015), where ATL spatial patterns are unknown outside of the sites with in situ measurements.

Analytical procedures exist to estimate ALT, such as the Stefan solution (Harlan and Nixon, 1978) or the Kudryavtsev equation. While the Stefan solution links the seasonal thaw depth to the accumulated surface thawing-degree days, the Kudryavtsev equation accounts for the effects of snow cover, vegetation, soil moisture, thermal properties and regional climate (Kudryavtsev et al., 1974; Yershov, 1998; Shiklomanov and Nelson, 1999). These methods, although accurate, are labor-intensive and limited in spatial coverage (Gangodagamage et al., 2014).

While traditional in situ measuring methods like probing with metal rods are very inefficient at the regional scale, remote sensing holds great potential to delineate ALT with continuous and larger spatial coverage. ALT can be derived by empirical relationships between probe measurements and a physical attribute measurable by remote sensing (Schaefer et al., 2015). Investigations have been made using the normalized difference vegetation index (NDVI) (McMichael et al., 1997; Kelley et al., 2004), digital elevation data and land cover classes (Nelson et al., 1997; Peddle and Franklin, 1993). Especially optical data have been used to retrieve vegetation characteristics (see Table 1). A combination with derivatives of digital elevation models (DEMs) has been shown to be of added value (Peddle and Franklin, 1993; Leverington and Duguay, 1996; Gangodagamage et al., 2014). Application of high-resolution optical satellite data in combination with high-resolution digital elevation data from airborne measurements have been shown to be useful for mapping ALT but are very limited in spatial extent. Subsurface thermal properties are also derived from land cover classes, but applicability has been demonstrated only for the permafrost transition zones so far (Bartsch et al., 2016).

Recently, subsidence rates have been used as input for modeling ALT (Schaefer et al., 2015). Synthetic aperture radar has been exploited using interferometric analyses (InSAR, which provides seasonal ground subsidence) in combination with soil properties to estimate ALT without using empirical relationships with probing data (Schaefer et al., 2015).

Most previous remote-sensing approaches (Leverington and Duguay, 1996; McMichael et al., 1997; Sazonova and Romanovsky, 2003; Schaefer et al., 2015) have utilized data with spatial resolutions of 30 m and coarser and been conducted in areas with shallow ALT (less than approximately 70 cm; see Table 1). Many regions such as the Yamal Peninsula are, however, characterized by a larger ALT range. Deeper active layers have been modeled by analytical approaches (e.g., Sazonova and Romanovsky, 2003) or by incorporating only a few ALT classes (e.g., Leverington and Duguay, 1996). For Yamal, previous tests indicate that ALT below 70, within the range of 70–100 and above 100 cm can be distinguished using NDVI (Leibman et al., 2015).

SAR backscatter intensity has so far not been investigated for ALT estimation. Radar backscatter at X-band is also related to vegetation coverage, especially shrubs (Duguay et al., 2015), due to volume scattering, similarly to the NDVI. The microwave signal interacts with leaves in the shrub canopy due to the comparably short wavelength (~ 3 cm). Leaf size of willows often exceeds this wavelength, and stems can have significantly larger diameters (Widhalm et al., 2016). Also vegetation water content may influence the return signal, but no dedicated investigations for tundra species exist. The overall backscatter intensity of a certain surface area is also influenced by surface roughness with respect to the wavelength, as well as by soil moisture. A higher moisture content leads to a higher dielectric constant and therefore higher backscatter values and additionally a reduction in penetration depth. X-band investigations in tundra (Lena Delta) suggest that such variations can occur (Zwieback et al., 2016), but results from Antonova et al. (2016) showed no sensitivity to precipitation over the same area.

In this study we hypothesize that there is a relationship between local ALT and X-band measurements, based on the influence of ALT affecting features on backscatter strength. Like ALT, backscatter is dependent on vegetation cover. Furthermore shrubs, which can be monitored with X-band data, can be related to snow cover due to their characteristic of retaining snow (Domine et al., 2016). Moreover the terrain in this region is closely linked to drainage and water content, which influence ALT. These characteristics in turn influence the predominant vegetation, which, including soil moisture, can be captured with microwave backscatter. We use in situ records from several sites in the proximity of a long-term-monitoring site on the Yamal Peninsula and discuss the results with respect to previous approaches which use remotely sensed information as a proxy for ALT.

2 Study area and datasets

2.1 The Vaskiny Dachi monitoring site

The Vaskiny Dachi research station (70°20′ N, 68°51′ E) was established in 1988 and is situated on the central Yamal Peninsula in a system of highly dissected alluvial-lacustrine-marine plains and terraces. It is located within a region of continuous permafrost where tundra lakes and river flood plains are the most prominent landscape features (Leibman et al., 2015). Dense dwarf shrubs (*Betula nana*) are widespread in the watersheds. Well-drained hill-

Table 1. Studies which used satellite data for determination of active-layer thickness (ALT): type of satellite data, accuracy and active-layer ranges.

Reference	Remotely sensed data	ALT measurement	Resolution	Study area	ALT	Accuracy
Peddle and Franklin (1993)	SPOT imagery (land cover) and photogrammetric DEM	In situ soil probing at regular intervals throughout field sample sites of 60 × 60 m	20 m	Ruby Range, southwest Yukon Territory, Canada	Classes: < 25 cm; 25–50 cm; > 50 cm; no permafrost	79 % agreement for the four classes
Leverington and Duguay (1996)	Landsat Thematic Mapper (NDVI, land cover) and DEM data	Pit measurements supplemented by three ground-probing measurements at 5 m intervals in four directions at each site	30 m	Mayo region, central Yukon Basin, Canada	Classes: < 70 cm; 70–150 cm; > 150 cm	93 % agreement for the three ALT classes
McMichael et al. (1997)	Landsat Thematic Mapper and handheld radiometer (NDVI)	Median of five ground-probing measurements at each sample point	30 m	Prudhoe Bay and Happy Valley, North Slope, Alaska	Average: < 35 cm	No relationship between NDVI and ALT on the Alaska North Slope in areas with little variation in relief. In areas where topography strongly controls the flow and redistribution of water, NDVI did account for approximately 40 % of the variability
Gangodagamage et al. (2014)	Lidar (local slope and landscape curvature) and Worldview-2 (NDVI)	Probing along transects of diverse length and at various intervals	2 m	Barrow, Alaska	20–70 cm	$R^2 = 0.76$ and RMSE ± 4.4 cm
Schaefer et al. (2015)	Subsidence from multiannual Phased Array type L-band Synthetic Aperture Radar (PALSAR)	Average of calibrated ground-penetrating radar (GPR) measurements within each pixel (∼ 40 traces per pixel); probe measurements at two CALM sites (1 × 1 km grid with 100 m interval, 10 × 10 m plot random point placement)	∼ 30 m	Barrow, Alaska	Average: 30–40 cm; < 40 cm in areas outside of drained lake basins	∼ 76 % of the study area within uncertainty of the used ground-penetrating radar and probing data (∼ 8 cm)

tops are occupied by dwarf-shrub–moss–lichen communities. On gentle poorly drained slopes, low shrubs and dwarf shrubs are well developed and mosses predominate. On convex tops and windy hill slopes, shrub–moss–lichen communities with spot-medallions are predominant. River valleys, thermocirques and landslide cirques with thick snow cover are characterized by willow thickets. Sedge and sphagnum bogs and flat-topped polygonal peatlands are common on flat and concave (saddles) surfaces of watersheds and terraces, in the river valley bottoms, on low lake terraces and in other depressions (Khomutov and Leibman, 2014).

The study area is characterized by continuous permafrost. ALT ranges between 40 cm in peat and up to 120 cm on sandy, poorly vegetated surfaces (Melnikov et al., 2004; Vasiliev et al., 2008; Leibman et al., 2011, 2012). There are extremes observed on high-centered sandy polygons, which can be 1–1.5 m high and up to 10 m in diameter, with an active layer exceeding 2 m. Spatial changes in ground temperature are controlled by the redistribution of snow which results from strong winds characteristic for tundra environments and the highly dissected relief of central Yamal (Dvornikov et al., 2015). The lowest ground temperature is characteristic for hilltops with sparse vegetation where snow is blown away. The warmest are areas with high willow shrubs, due to the retention of snow, found on slopes, in valleys and lake depressions. While the spatial distribution of ALT depends on lithology and surface covers, temporal fluctuations are controlled by ground temperature, summer air temperature and summer precipitation (Leibman et al., 2015).

2.2 In situ measurements

In 1993 a Circumpolar Active Layer Monitoring (CALM) site was established at Vaskiny Dachy, placed on the top and slope of a highly dissected plain affected by landslides, with sandy to clayey soils. The CALM program, designed to observe the response of the active layer and near-surface permafrost to climate change, currently incorporates more than 100 sites. The International Permafrost Association serves as the international facilitator for the CALM network, which is now part of the WMO Global Terrestrial Network for Permafrost (GTN-P) (Brown et al., 2000).

Within the Greening of the Arctic (GOA) project of the International Polar Year (IPY), which was funded by NASA's Land-Cover and Land-Use Change (LCLUC) Program, three additional monitoring sites were established in the Vaskiny Dachi area (Walker et al., 2009). Study sites were established within areas with more or less homogeneous vegetation. The site Vaskiny Dachi-1 (VD-1) has clay soils, and the vegetation is heavily grazed sedge and dwarf-shrub–moss tundra. Soils at Vaskiny Dachi-2 (VD-2) are a mix of sand and clay; its vegetation is heterogeneous but dominated by dwarf birch, small reed grass and sedge, cowberries and mosses. At Vaskiny Dachi-3 (VD-3) the soils are sandy and the vegetation is a dry dwarf-shrub–lichen tundra (Walker et al., 2009).

The ALT is measured by a metal probe according to CALM protocol. This involves a late-season mechanical probing, in this case late August, when ALT is near its end-of-season maximum. A 1 cm diameter graduated steel rod is inserted into the soil to the depth of resistance to determine the depth of thaw (Brown et al., 2000).

ALT is measured at a spacing of 10 m within the 100×100 m grid at the CALM site, resulting in 121 measuring points. The VD sites each feature five transects. At VD-1 and VD-2 these transects form grids of 50×50 m. Transects are 12.5 m apart, and ALT is measured every 5 m, resulting in 55 measurement points per site. The transects at VD-3 are arranged in areas of homogeneous vegetation (Walker et al., 2009). The site of VD-3 features higher ALT values, most likely because of the present sandy soils, which yield a greater conductivity and water permeability (higher convective heat exchange). The CALM grid site is far more heterogeneous than the other VD sites and holds patches of dry cryptogam crust, grasses and mosses; low and high shrubs; and some wet sedge spots. Cryptogam crust is encountered at the concave hilltop, while high shrubs were mostly located at the landslides (Fig. 8). Here, ALT is locally higher due to the high salinity of clayey deposits which contain no ice under negative temperature and do not resist to probing.

In August 2015, we carried out a dedicated vegetation survey of each CALM grid point, where we determined the dominant vegetation cover within a 3×3 m area (Fig. 1). The following classes are distinguished: cryptogam crust, low shrubs (< 15 cm), medium shrubs (15–30 cm), high shrubs (> 30 cm), grass and moss, a class where sedges dominate and classes of mixed vegetation. Further information on vegetation has been collected outside of the ALT measurement sites in August 2014. Over 60 points were registered, but only 36 of these points could be further used because of low homogeneity with respect to the spatial resolution of the satellite data. This survey included the most dominant classes of the region and therefore covered more types than can be found at the VD sites or the CALM grid: low shrubs (< 20 cm), medium shrubs (20–60 cm), high shrubs (> 60 cm), cryptogam crust, and a mixture of grasses and sedges.

Furthermore we conducted moisture measurements at the CALM grid. We used the Delta-T WET Sensor with a handheld HH2 Moisture Meter to measure the moisture content of the top 5 cm at each grid point on three dates in August 2015.

2.3 X-band data

X-band data have so far been used to investigate surface deformations like thaw subsidence and frost heave (Beck et al., 2015; Zhang et al., 2016; Wang et al., 2016), to monitor tundra shrub growth (Duguay et al., 2015) or to date drained thermokarst lake basins (Regmi et al., 2012) related to permafrost research.

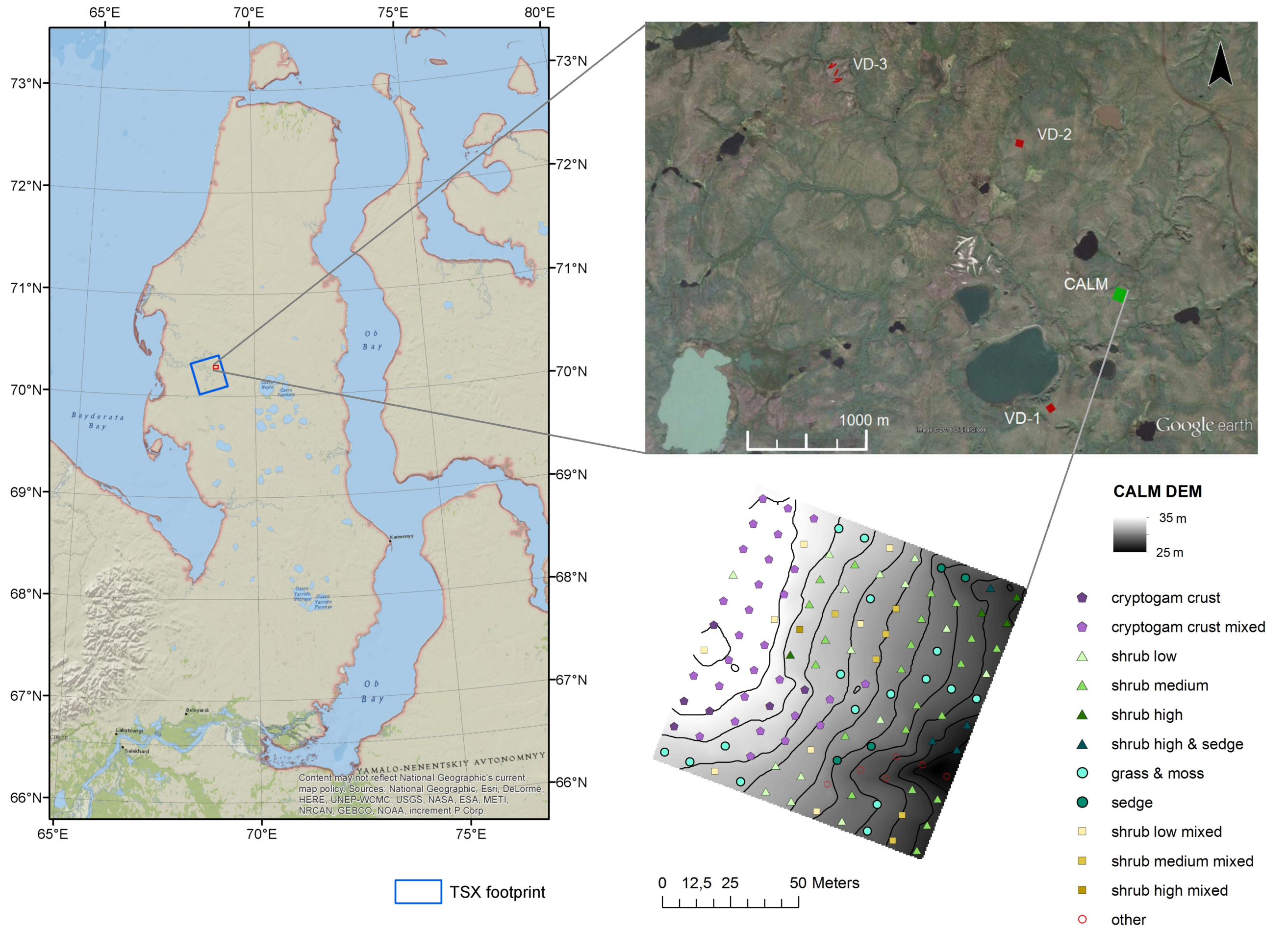

Figure 1. Location of the study area (with monitoring sites Vaskiny Dachi (VD) 1–3 and CALM gird) within the Yamal Peninsula and CALM grid DEM with land cover information (sources left: ArcMap Basemaps: National Geographic, Esri, DeLorme, HERE, UNEP-WCMC, USGS, NASA, ESA, METI, NRCAN, GEBCO, NOAA, Increment P Corp. Source top right: Google Earth, Image © 2016 Digital Globe. Bottom right: DEM (Dvornikov et al., 2016), land cover information from vegetation survey of August 2015).

Backscatter information from data of the TerraSAR-X mission have been used for this study. The digital elevation model available from the TanDEM-X mission has been used as an auxiliary dataset for TerraSAR-X data preprocessing.

The German national SAR satellite system TerraSAR-X is based on a public–private partnership agreement between the German Aerospace Center (DLR) and EADS Astrium GmbH. It was launched in June 2007 and started its operational service at the beginning of 2008 (DLR, 2009). The satellite flies in a sun-synchronous, dawn–dusk orbit with an 11-day repeat period. TerraSAR-X features an advanced high-resolution X-band synthetic aperture radar with a center frequency of 9.65 GHz, corresponding to a wavelength of about 3.1 cm. TerraSAR-X operates in SpotLight, StripMap and ScanSAR mode with various polarizations. In this study HH (horizontally sent and horizontally received) polarized images of StripMap mode were used, which image strips of 30 km width at 3 m resolution (Werninghaus et al., 2004).

Six images from August 2014 and 2015 (three images per year) were obtained as SSC (single-look slant range complex) and have been acquired in the same ascending orbit and beam (incidence angle range 27.3–30.3°).

The TanDEM-X mission is an extension of the TerraSAR-X mission, co-flying a second satellite of nearly identical capability in a close formation. This enables the acquisition of highly accurate cross- and along-track interferograms without the inherent accuracy limitations imposed by repeat-pass interferometry due to temporal decorrelation and atmospheric disturbances (Krieger et al., 2007). In this study the TanDEM-X Intermediate DEM (IDEM, ~ 12 m pixel spacing, < 10 m absolute horizontal and vertical accuracy) was used for terrain correction, which, compared to the final TanDEM-X DEM product, might have limitations with respect to product quality and completeness (Wessel, 2013).

2.4 Landsat data

Landsat 8, launched in 2013, is a NASA (National Aeronautics and Space Administration) and USGS (Department of the Interior U.S. Geological Survey) collaboration, which extends the 40-year Landsat record. It carries two sensors, the Operational Land Imager (OLI) and the Thermal Infrared Sensor (TIRS), whose spectral bands remain comparable to the Landsat 7 Enhanced Thematic Mapper Plus (ETM+) and operate in the visible, near infrared, shortwave and thermal infrared. Landsat 8 flies in a near-polar, sun-synchronous 705 km circular orbit and acquires data in 185 km swaths segmented into 185 km × 180 km scenes. For this study two Level 1 terrain-corrected (L1T) scenes of 22 July 2014 and 10 August 2015 were obtained in order to calculate NDVI (spatial resolution: 30 m) and compare the already-established approach of using NDVI for ALT delineation to the approach introduced in this study of utilizing TerraSAR-X backscatter.

3 Methodology

In microwave remote sensing the radar backscatter is dependent on sensor parameters like incidence angle, polarization and wavelength and also on geometric parameters such as surface roughness and vegetation structure, as well as soil properties. Shorter wavelengths do not penetrate as much as longer wavelengths into vegetation and soil; therefore short wavelengths like X-band rather yield information about the upper layers of vegetation (Ulaby et al., 1982). The assumption for this study is that surface roughness variations play a minor role regarding spatial backscatter differences across the study site. Backscatter increases with increasing vegetation height for X-band in tundra, which originates from volume scattering and double bounce (leading to higher backscatter) rather than surface roughness (Ullmann et al., 2014). It can be also expected that soil moisture variations are not reflected in X-band measurements when vegetation cover is present. The assumption is that volume scattering and double bounce in vegetation are the main contributors to spatial differences in backscatter. Several studies have exemplified the separability of tundra shrubs from their surroundings (Ullmann et al., 2014; Duguay et al., 2015). In Antonova et al. (2016) it is shown that X-band time series analysis allows for a clear discrimination of major landscape elements in tundra regions.

The local vegetation patterns are influenced by terrain and soil moisture and also correlate with snow cover thickness, which are all ALT-influencing factors (Shiklomanov and Nelson, 1999; Gomersall and Hinkel, 2001; Kelley et al., 2004). Areas with shrubs have higher snow cover, which prevents the ground from cooling in the winter. The ALT might therefore also be higher than in the surrounding area. Based on results of previous studies which utilized the vegetation index NDVI (Table 1) and the mutual dependency of NDVI and radar backscatter on vegetation coverage, it is expected that a relationship between X-band backscatter measurements and ALT is given. We compiled a dataset based on TerraSAR-X which allows the investigation of this relationship. This included for SAR common preprocessing steps to account for variations due to viewing geometry.

Six TerraSAR-X images from August 2014 and 2015 were processed (three images per year). It is assumed that within this time stable phenological conditions can be expected. Utilizing the software NEST (Next ESA SAR Toolbox), range–Doppler terrain correction was performed with a TanDEM-X Intermediate DEM (∼ 12 m resolution) in order to orthorectify the images and to compensate for distortions due to topographical variations and the tilt of the sensor. Images were processed to a pixel spacing of 2 m, and a radiometric normalization was applied to account for incidence-angle-dependent sensitivity. The so-called resulting σ_0 values were then converted into decibels. The term backscatter refers in the following to these values, which represent the normalized measure of the radar return. SAR data are affected by so called speckle, which is a noise-like effect. It can be understood as an interference phenomenon due to a number of scatterers within each resolution cell. The images were therefore further averaged over time, and a spatial filter (average value of the cells in the neighborhood was calculated: 5 × 5 cells – 10 m) was applied to subdue this noise.

Backscatter and NDVI values for the sites VD-1, VD-2 and VD-3 were extracted and compared to the mean ALT values of 2014 and 2015 of each measuring point. The relationship of backscatter values and ALT was examined by varying representations. Box plots for ALT classes and for backscatter classes are shown in Fig. 4. ALT values were separated into 10 cm classes, and the backscatter classes ranged 1 dB, allowing a representative number of sampling points per class (7 and 13 points minimum per class, respectively). σ_0 values as well as NDVI values were additionally compared directly to ALT by scatterplots (Fig. 5). Fitted linear functions were applied to characterize the relationship between TerraSAR-X backscatter and NDVI as well as ALT values of the sites VD-1, VD-2 and VD-3. The coefficient of determination ($R^2 = 1 - \frac{\sum(y_i - f_i)^2}{\sum(y_i - \bar{y})^2}$, the proportion of the variance in the dependent variable that is predictable from the independent variable) was calculated for the regression lines which involved all VD sites, as well as for regression lines for each VD site separately (Table 2). Validation has been undertaken using ALT measurements at the CALM grid. Root mean square error (RMSE) was calculated, representing the modeled ALT (linear regression of all VD sites) versus the measured ALT at the CALM site. Moreover χ^2 was determined, which also accounts for observational uncertainties. An observational uncertainty of 4 cm was assumed for the probe measurements, which has been investigated by Leibman (1998) for sandy soils (2–4 cm) in this region. The mod-

Table 2. R^2 between X-band backscatter and NDVI (22 July 2014 and 10 August 2015) and ALT. R^2 has been calculated for all calibration sites combined (VD-1,2 and 3) and separately (ALT range for VD-1: 56–108 cm; VD-2: 45–102 cm; VD-3: 90–140 cm). RMSE values represent the modeled ALT (linear regression of sites VD-1, VD-2 and VD-3) versus the measured ALT at the CALM site. χ^2 statistics compare the modeled and measured ALT at the CALM site under consideration of observational uncertainties.

Dataset	R^2 (VD-1, 2 and 3)	RMSE (cm) (CALM)	χ^2 (cm) (CALM)	R^2 (VD-1)	R^2 (VD-2)	R^2 (VD-3)
TerraSAR-X	0.656	20	25	0.143	0.153	0.622
TerraSAR-X (exclusion of points with high variability)	0.712	21	27	0.172	0.167	0.622
NDVI 22 July 2014	0.734	27	46	0.171	0.016	0.017
NDVI 10 August 2015	0.746	30	57	0.002	0.130	0.002

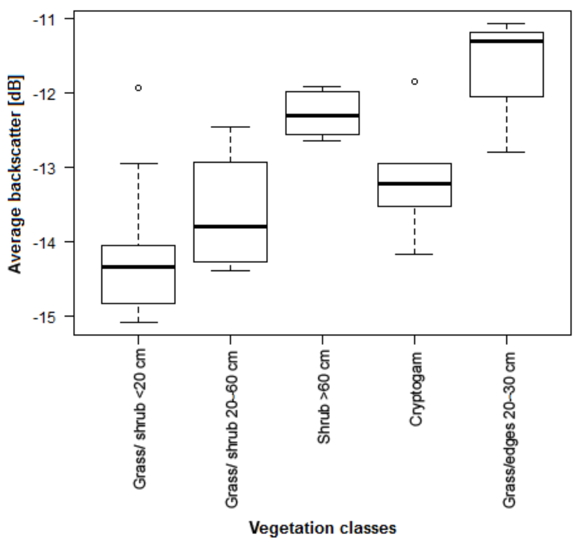

Figure 2. Box plot for backscatter values of various vegetation types. The points used were recorded within a field campaign in 2014. Backscatter values were extracted from the temporally averaged and spatially filtered image of August 2014 and 2015 acquisitions.

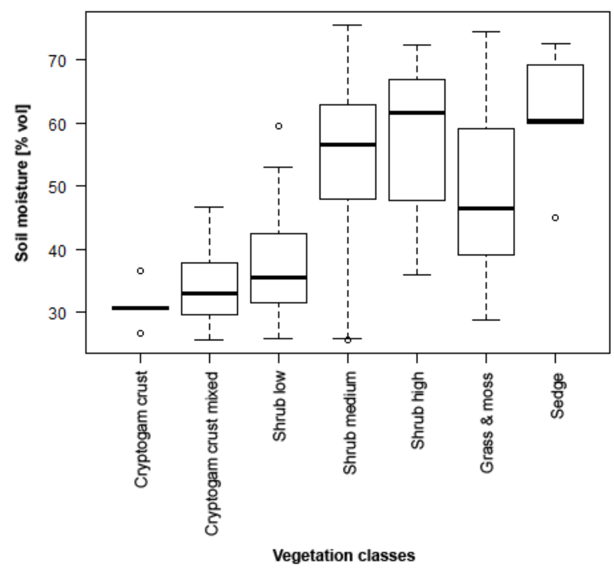

Figure 3. Box plot for mean soil moisture values of three acquisition dates in late August 2015 for vegetation types at the CALM grid.

eled and measured ALT values at the CALM grid were further compared by scatterplots depicting the different vegetation types (Fig. 7) in order to investigate their impact.

Backscatter statistics have also been derived for different vegetation classes from locations of the 2014 survey outside of the ALT measurement sites (Fig. 2). These locations represent relatively homogeneous sites (with respect to TerraSAR-X spatial resolution). The ALT sites, especially the CALM grid, are comparably heterogeneous and therefore of limited applicability for determination of backscatter dependence on vegetation type. The relation of vegetation type and soil moisture was examined for the CALM grid using moisture measurements of August 2015 (Fig. 3).

4 Results

The assumption that backscatter increases with increasing amount of vegetation could be confirmed for the Vaskiny Dachi area (Fig. 2). There is a difference of about 2 dB between the median for shrubs less than 20 cm and those larger than 60 cm. σ_0 values for the grass–sedge class do, however, exceed these values. Cryptogam crust backscatter is on the same order of magnitude as shrubs between 20 and 60 cm height. Although the sparse vegetation in these areas consists mostly of lichen and volume scattering within is negligible, these spots often show higher surface roughness or even hummocks, which may lead to a rise in backscatter amount. The box plot of Fig. 3, which shows the relationship between soil moisture and vegetation types at the CALM grid, reveals that the lowest soil moisture is encountered for areas with

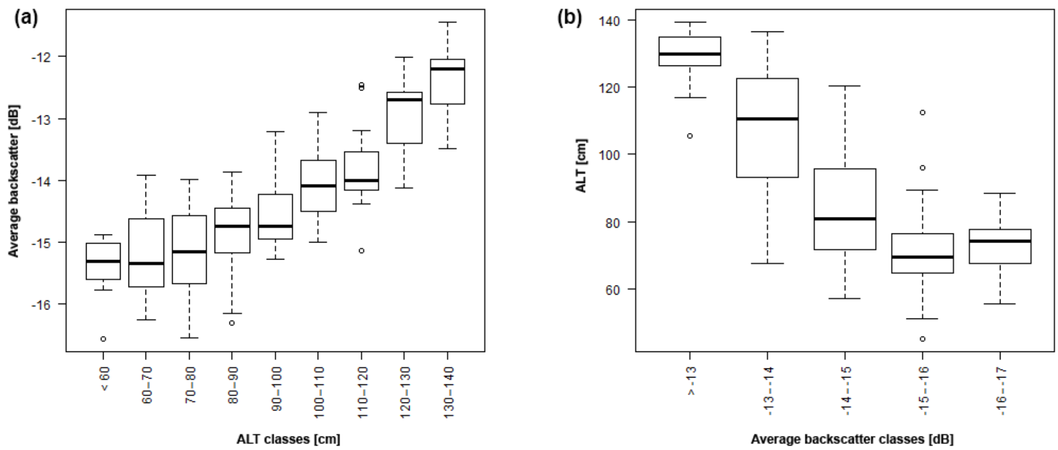

Figure 4. Box plots showing median, minimum and maximum values; first and third quartile and outliers of the ALT; and backscatter values of the sites VD-1, VD-2 and VD-3. Left: σ_0 statistics for ALT classes (10 cm). Right: ALT statistics for backscatter classes (1 dB).

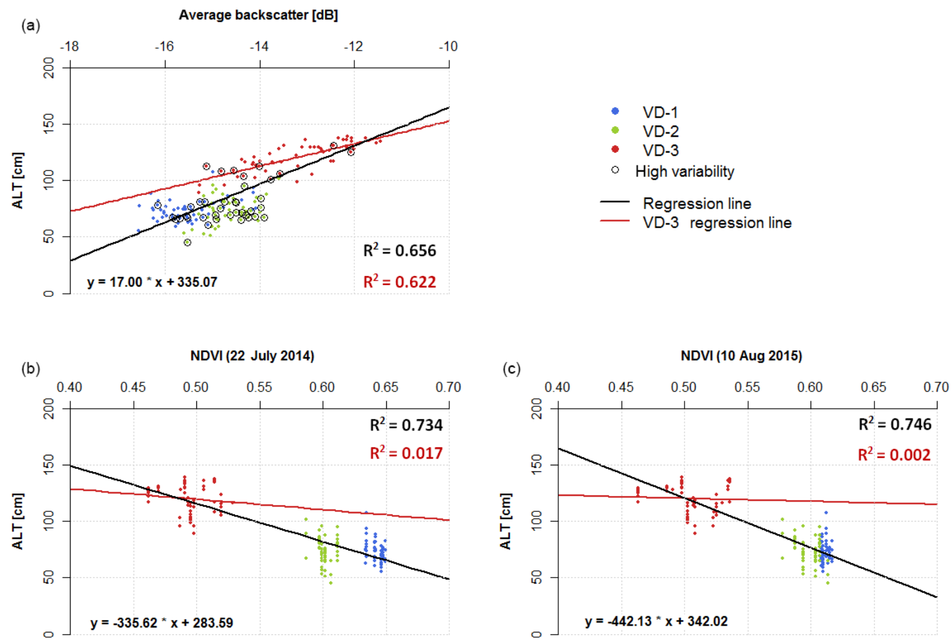

Figure 5. Upper left: comparison between σ_0 and ALT values at the sites VD-1 to VD-3. Points with differences of more than 1 dB between 2014 and 2015 are marked by circles. Linear regression for σ_0 and ALT values of all sites in black and for site VD-3 in red. Bottom: comparison between NDVI (22 July 2014 and 10 August 2015) and ALT values at the sites VD-1 to VD-3. Linear regression for NDVI and ALT values of all sites in black and for site VD-3 in red.

cryptogam crust, while higher shrubs and especially sedges dominate in areas of high soil moisture.

Class statistics (Fig. 4) indicate a relationship between σ_0 and larger thaw depths. Low backscatter values dominate in areas with low ALT, and high backscatter values coincide with high ALT. However, the median σ_0 for shallow ALT does not decrease with decreasing ALT at the same rate as for deeper ALT. The scatterplots of the filtered σ_0 and ALT values of the sites VD-1 to VD-3 also indicate this correlation (see Fig. 5). It also becomes apparent that the change in slope that is visible in the box plot of Fig. 4 is caused by different backscatter values of the sites VD-1 and VD-2 (Fig. 5). Nevertheless σ_0 increases generally with increasing ALT. The overall higher ALT values of VD-3 are reflected by their higher backscatter values. A range of 5 dB can be observed for an ALT range of 100 cm (40–140 cm).

A coefficient of determination of 0.66 was obtained for the linear regression of backscatter and ALT values (see Table 2). The mathematical form of the regression line is given in Fig. 5. The standard error of the intercept is 14.00 and

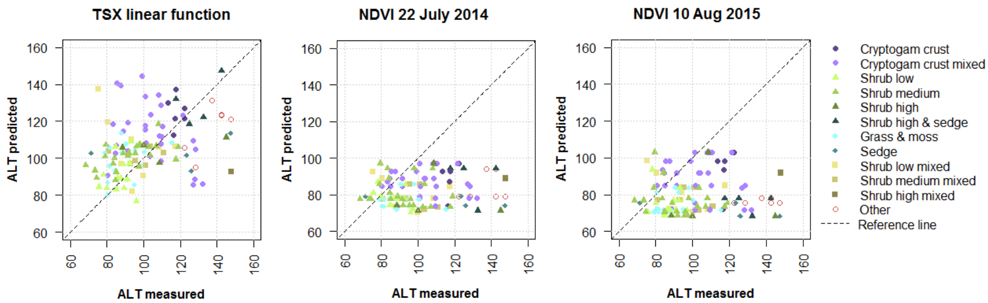

Figure 6. Comparison between predicted and measured ALT values at the CALM grid with differentiation between vegetation types for TerraSAR-X and NDVI approaches.

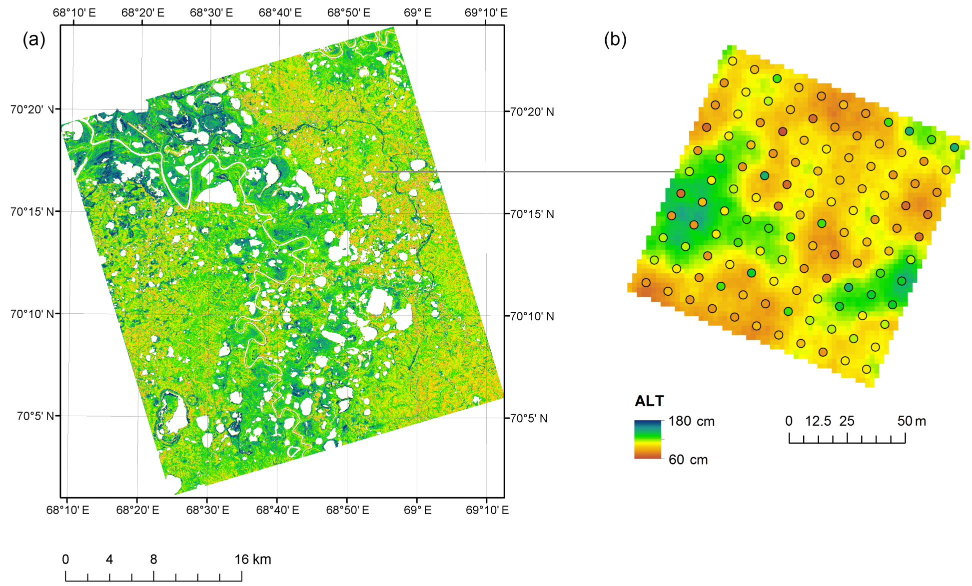

Figure 7. Left: calculated ALT map for all TerraSAR-X scenes, based on TerraSAR-X backscatter values. Right: calculated ALT map (background raster, based on X-band backscatter) for the CALM grid compared to in situ measurements (circles).

0.96 for the slope, respectively. R^2 for the individual VD sites showed higher values for VD-3 than for VD-1 and VD-2, which both feature lower ALT values. The linear regression which incorporated all calibration sites (VD-1, VD-2 and VD-3) yielded an RMSE of 20 cm at the CALM grid site and 25 cm for χ^2. Some VD points showed a backscatter variability of more than 1 dB between the acquisitions of 2014 and 2015. An exclusion of these points would slightly increase the coefficients of determination, but no positive effect could be found with RMSE values at the CALM grid.

The relationship found between TerraSAR-X backscatter and ALT is not as pronounced at the CALM validation site as at the other plots. In particular, a patch at the highest elevation of the CALM grid was expected to show higher ALT values according to the calculations from the satellite data (Figs. 7 and 6). There are also some spots with slightly higher ALT than predicted. This applies to ALT larger than 125 cm. With the exception of the area around the hilltop, the patterns derived with TerraSAR-X resemble those of the in situ measurements.

A deeper active layer can be found in areas with high shrubs as well as cryptogam crust at the CALM site (see Fig. 6). Extremes of ALT can further be encountered at the clay-rich landslides with relatively sparse vegetation, classified as "other" in Fig. 6. Thinner active layers were encountered at zones with grass and moss or low shrubs (see Fig. 6). Residuals increase for depths larger than 125 cm, especially in case of dominance of cryptogam crusts.

In Fig. 7 a map of the calculated ALT is given for the entire TerraSAR-X scene (open water bodies are masked out). Linear features are expected to be false values as they can be attributed to artificial objects. They show low as well as high ALT values depending on surface roughness and material (air strip and rail track, respectively). Values across the scene range between 60 and 180 cm. ALT is higher in drained or partially drained lake basins.

Derived scatterplots of NDVI and ALT values also reveal a relationship within the observed NDVI range of 0.46–0.65 (Fig. 5). The standard error of the intercept is 9.21 for 22 July 2014 and 11.60 for 10 August 2015, and 15.80 and 20.21 for the slope, respectively. Both NDVI images showed even larger coefficients of determination (about 0.73–0.75) than the TerraSAR-X approach (Table 2). The achieved RMSE at the validation site is, however, about 7 cm larger than when using the TerraSAR-X backscatter values. Furthermore, when using only site VD-3, which has the highest range and total thickness of the active layer, comparable to the values at the CALM grid, the linear regression for the backscatter values has a coefficient of determination of 0.622, while for NDVI values it is only 0.017 and 0.002, respectively (Fig. 5). The NDVI-derived ALT values for the CALM site range at most between 70 and 100 cm for 22 July 2014 and between 60 and 110 cm for 10 August 2015, while measured values have a range of 60–150 cm.

5 Discussion

The assumption that X-band backscatter variations result mostly from differences in volume scattering in vegetation over tundra does not seem to be valid for the selected sites. Radar backscatter is dependent on volume scattering, surface roughness and soil moisture. The influence of all these effects can be perceived in Fig. 2. For shrubs a major contributor to backscatter is the volume scattering that takes place within the vegetation. A rise in volume indicated by shrub height clearly gives rise to backscatter amount. This effect is also described in Duguay et al. (2015), where areas with high shrubs show higher backscatter values. A pronounced relationship was, however, not found for X-band in HH by Ullmann et al. (2014) over the MacKenzie Delta. They applied a smaller spatial filter of 3×3 and used data from the end of the growing season (mostly September) when plant decay is already expected to take place. A season-related reduction of leaves on shrubs could lead to a decrease in volume scattering and therefore lower backscatter values. The magnitude of backscatter for cryptogam crust, which predominantly occurs on sandy soils, can be attributed neither to volume scattering in vegetation nor to soil moisture (Figs. 2 and 3). Surface roughness or partial interaction within the upper soil may lead to higher backscatter than for grass and low shrubs < 20 cm.

High soil moisture is typical for the class sedges (Fig. 3), giving rise to the backscatter amount. Additionally the so called double bounce effect, which may occur for sedges and grass in standing water, can lead to an increase of received backscatter (Fig. 2).

Using backscatter intensity at only one polarization (as available for this study) does not allow distinguishing between surface and volume scattering. Polarimetric analyses (using other combinations of H and V polarizations) may help to distinguish the scattering mechanism contributions (see e.g. Ullmann et al., 2014). Data acquired at different polarizations are, however, not available for the study site.

The above described influences on radar backscatter can be linked to ALT-controlling factors. The effect of shrubs on ALT has been described contradictorily by different authors. On the one hand shrubs have been said to have a cooling effect due to shading in the summer (Blok et al., 2010; Lawrence and Swenson, 2011; Pearson et al., 2013), leading to shallower ALT. In other publications (Domine et al., 2016; Myers-Smith and Hik, 2013) shrubs have been linked with ground warming due to the isolating effect of snow cover. Shrubs trap wind-blown snow and limit snow erosion by wind. It seems that the prevailing effect of cooling or warming may be caused by the length of the winter or summer season. For the CALM site it can be shown that shrubs coincide with deeper ALT (Fig. 6). However it needs to be noted that shrubs are found here on saline clay, which, as stated before, can lead to higher ALT values measured by probing. In clayey saline soils (with ALT values > 130 cm at the CALM site) the freezing point is different from zero and probes can be inserted to greater depths (Leibman, 1998).

Soil moisture is another factor that influences microwave backscatter and ALT. It increases the backscatter amount due to the rise of the dielectric constant. It may also lead to higher ALT, caused by an increased heat flux and an enhanced conductive transfer of heat into subsurface layers (Gross et al., 1990; Shiklomanov et al., 2010). For the Yamal region the measured moisture content is influenced strongly by lithology. While sandy soils are found to be dry, clayey saline soils often hamper infiltration and show higher soil moisture or even standing water. Although barren sandy areas are dryer, they have been shown to have maximal ALT (Leibman et al., 2015) due to higher heat flux, increased by infiltration of rain water. Cryptogam crust is typically found on high-centered sandy polygons in the study area. For these points the following restrictions of the used approach become apparent. Most points for which the modeled ALT shows high deviations from the in situ data have or lie close to spots of cryptogam crust. The volume scattering for areas with cryptogam crusts is expected to be very low (as described in the Sect. 4), but the recorded σ_0 is comparable to medium shrub heights which have a lower thaw depth. The higher σ_0 values could be due to higher surface roughness. The moisture content itself may also contribute to σ_0; however soil moisture values for areas with cryptogam crust have been shown to be very low (see Fig. 3). Heterogeneity regarding vegetation coverage may also contribute. Especially sites with mixed types show high deviations (see Fig. 6).

The redistribution of water and consequently also the occurring vegetation is controlled not only by lithology but also by topography (see Fig. 8), which has been shown to be useful in delineating ALT (Peddle and Franklin, 1993; Leverington and Duguay, 1996; Gangodagamage et al., 2014). Although we did not use topographic information in our study

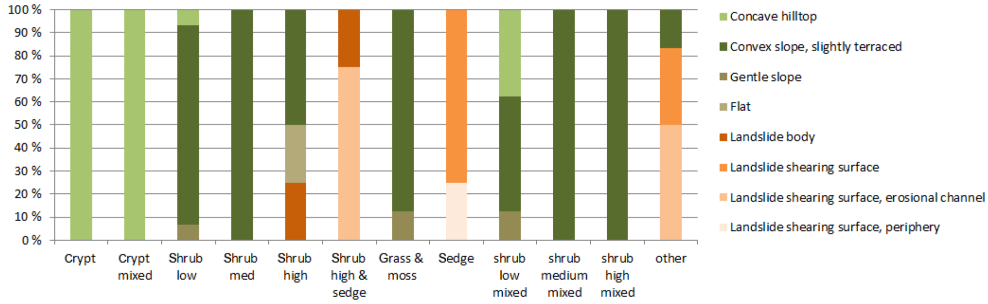

Figure 8. Comparison of topographic units (source CALM metadata, Earth Cryosphere Institute, Siberian Branch of the Academy of Sciences (SB RAS)) and vegetation type (survey of August 2015) at the CALM grid, illustrating the interrelation of certain topographic features and specific vegetation covers.

in order to derive ALT, it is indirectly introduced into our measurements through its effects on vegetation and moisture. For future studies the potential of refining the backscatter approach by incorporating topographic information could be explored.

The comparison of the produced ALT map to the ALT measurements at the CALM grid showed that some points within the validation dataset from the CALM grid are not well represented by the map (Fig. 7). These sites also deviate in the probe data. For instance for one of these points an ALT of > 170 cm was measured in 2014, which is about almost double the values of the surrounding points, and in 2015 only 116 cm was registered. Such an extreme variability of ALT could be explained by an interface between a sandy active layer and a clayey permafrost at this location.

Regarding the delineated ALT map for the entire TerraSAR-X scene (Fig. 7), it needs to be considered that neither the calibration data (VD sites) nor the validation site (CALM grid) included lowlands with extensive wetlands, as can be found in this region. Because of the lack of ALT measurements for these areas, the shown map is only representative for parts of the region, while lowlands would need further verification and could be masked out using a DEM. The higher ALT in drained lake basins does agree with findings of Schaefer et al. (2015) around Barrow. They, however, argue that their algorithm actually overestimates ALT at these locations.

The comparison of Landsat-8-derived NDVI values and ALT revealed a negative correlation (see Fig. 5), which is contrary to most studies of other regions (Gangodagamage et al., 2014; McMichael et al., 1997). However Leibman et al. (2015) previously obtained similar results for the Yamal region at the CALM grid. Results suggest that NDVI is higher for sites with grasses, mosses and sedges than for medium to high shrubs (Salix), although the near infrared used is influenced by plant cell structure and vegetation biomass. These shrubs do, however, coincide with very wet soils (Fig. 3) and are growing within partially waterlogged depressions. The sensitivity of NDVI to water (Raynolds and Walker, 2016) might have an impact over these sites. Furthermore a difference between the training datasets becomes apparent. Both VD-1 and VD-2 lie within a similarly lower ALT range, but especially the acquisition of 22 July 2014 shows clearly higher NDVI values for VD-1 than for VD-2. This points to different vegetation types. A difference is also observed for the X-band backscatter, where VD-1 shows slightly lower backscatter values than VD-2. The backscatter differences could be explained by a slightly higher surface roughness, which is, however, not pronounced enough to have a sufficient influence on the site's snow cover or even ALT. Moreover vegetation at VD-2 is rather heterogeneous and also includes patches of sedges or reeds, which could increase the amount of backscatter. While VD-1 and to a small amount even VD-3 also shows sedge vegetation, these sandier sites show a different kind of grass (*Carex bigelowii* instead of *Calamagrostis holmii*). Moreover a clear difference between Landsat acquisitions of 22 July 2014 and 10 August 2015 exists due to differences in vegetation and their respective phenological cycles (Bratsch et al., 2016), which are in turn influenced by terrain features and consequent draining conditions.

The advantages and disadvantages of the new approach with respect to previous studies could be demonstrated by application of the NDVI approach over the same site and using the same training dataset. Investigations presented in this paper showed that the introduced approach of using TerraSAR-X backscatter values to delineate ALT values is suitable to provide estimates higher than 30 m resolution over unsaturated soils with ALT ranging from 40 to 140 cm in areas outside of high-centered sandy polygons. One previous study that was conducted within comparable ALT ranges used NDVI and land cover information derived from Landsat data in combination with DEM data to derive three classes of ALT (Leverington and Duguay, 1996). A 93 % agreement rate for three different ALT classes was obtained. In contrast to our study, Leverington and Duguay (1996) used "best-estimate" ALT values from either a pit value or the average of pit and probe measurements, and fixed ALT classes. In our study we used measurements for single points from grid points within a 100 × 100 m raster of high heterogeneity. All but one measured ALT value fall into only one ALT class (70–150 cm) used by Leverington and Duguay (1996). The given accuracy can therefore not be compared.

The used TerraSAR-X data have been acquired in StripMap mode, which has a swath width of 30 km. This sensor can, however, also acquire data over 270 km when using the Wide ScanSAR mode (40 m resolution). This would allow the transfer of the approach to larger regions. The incidence angle range investigated thus far is, however, very limited. Differences in the described backscatter–ALT relationship due to incidence angle effects would need to be considered.

6 Conclusions

The common dependency of ALT and X-band backscatter values (HH, approximately 30° incidence angle) on land cover types as well as the interrelation of terrain, vegetation, soil moisture and snow cover yields a correlation which can be used to derive ALT with an RMSE of 20 cm over a long-term-monitoring site in central Yamal. It can be shown that in general higher ALT values correspond with higher backscatter values for the tested ALT range of 40–140 cm. The accuracy is lower over sites with mixed vegetation types within the pixels. Especially contributions from areas with little vegetation (cryptogam crusts) alter the relationship between backscatter and ALT. Soil moisture and/or surface roughness influence the signal over these sites. Polarimetric SAR analyses which allows distinguishing different scattering mechanisms might be suitable to tackle these issues. This could, however, not be tested due to unavailability of such satellite data. Results indicate a better performance than NDVI for higher ALT, but investigations with higher-spatial-resolution optical data would be required for confirmation.

7 Data availability

ALT information of the CALM site is available via GTNP or via the following link: https://www2.gwu.edu/~calm/data/webforms/r5_f.html (Leibmann, 2016). Soil moisture and temperature measurements as well as mean backscatter values for the CALM points will be provided via https://www.pangaea.de/.

Author contributions. Barbara Widhalm performed all data analyses, collected moisture and vegetation information at the CALM site, and compiled the manuscript. Annett Bartsch contributed to the development of the concept of the approach as well as to the manuscript. Marina Leibmann and Artem Khomutov collected the active-layer measurements at the long-term-monitoring sites as well as the vegetation information at sites outside of the ALT monitoring sites and contributed to the interpretation and discussion of the results.

Competing interests. The authors declare that they have no conflict of interest.

Acknowledgements. This work was supported by the Austrian Science Fund under grant [I 1401] and the Russian Foundation for Basic Research grant 13-05-91001-ANF-a (joint Russian–Austrian project COLD-Yamal). TerraSAR-X data were made available by DLR through PI agreement LAN1706 and HYD2522, and Tandem-X data through HYDR0226.

Edited by: A. Kääb
Reviewed by: two anonymous referees

References

Antonova, S., Kääb, A., Heim, B., Langer, M., and Boike, J.: Spatio-temporal variability of X-band radar backscatter and coherence over the Lena River Delta, Siberia, Remote Sens. Environ., 182, 169–191, doi:10.1016/j.rse.2016.05.003, Remote Sens. Environ., 2016.

Bartsch, A., Höfler, A., Kroisleitner, C., and Trofaier, A. M.: Land Cover Mapping in Northern High Latitude Permafrost Regions with Satellite Data: Achievements and Remaining Challenges, 8, 979, doi:10.3390/rs8120979, 2016.

Beck, I., Ludwig, R., Bernier, M., Strozzi, T., and Boike, J.: Vertical movements of frost mounds in subarctic permafrost regions analyzed using geodetic survey and satellite interferometry, Earth Surf. Dynam., 3, 409–421, doi:10.5194/esurf-3-409-2015, 2015.

Blok, D., Heijmans, M. M. P. D., Schaepman-Strub, G., Kononov, A. V., Maximov, T. C., and Berendse, F.: Shrub expansion may reduce summer permafrost thaw in Siberian tundra, Glob. Change Biol., 16, 1296–1305, doi:10.1111/j.1365-2486.2009.02110.x, 2010.

Bratsch, S., Epstein, H., Buchhorn, M., and Walker, D.: Differentiating among Four Arctic Tundra Plant Communities at Ivotuk, Alaska Using Field Spectroscopy, Remote Sensing, 8, 51, doi:10.3390/rs8010051, 2016.

Brown, J., Hinkel, K. M., and Nelson, F. E.: The circumpolar active layer monitoring (CALM) program: Research designs and initial results, Polar Geography, 24, 3, 2000.

DLR: TerraSAR-X Mission, brochure, Bonn-Oberkassel, Germany, 2009.

Domine, F., Barrere, M., and Morin, S.: The growth of shrubs on high Arctic tundra at Bylot Island: impact on snow physical properties and permafrost thermal regime, Biogeosciences, 13, 6471–6486, doi:10.5194/bg-13-6471-2016, 2016.

Duguay, Y., Bernier, M., Lévesque, E., and Tremblay, B.: Potential of C and X Band SAR for Shrub Growth Monitoring in Sub-Arctic Environments, Remote Sensing, 7, 9410–9430, doi:10.3390/rs70709410, 2015.

Dvornikov, Y., Khomutov, A., Mullanurov, D., Ermokhina, K., Gubarkov, A., and Leibman, M.: GIS and field data based modelling of snow water equivalent in shrub tundra, Fennia, 193, 53–65, doi:10.11143/46363, 2015.

Dvornikov, Y., Leibman, M., Heim, B., Bartsch, A., Haas, A., Khomutov, A., Gubarkov, A., Mikhaylova, M., Mullanurov, D., Widhalm, B., Skorospekhova, T., and Irina, F.: Geodatabase and WebGIS project for long-term permafrost monitoring at the Vaskiny Dachi research station, Yamal, Russia, Polarforschung, 85, 107–115, doi:10.2312/polfor.2016.007, 2016.

Gangodagamage, C., Rowland, J. C., Hubbard, S. S., Brumby, S. P., Liljedahl, A. K., Wainwright, H., Wilson, C. J., Altmann, G. L., Dafflon, B., Peterson, J., Ulrich, C., Tweedie, C. E., and Wullschleger, S. D.: Extrapolating active layer thickness measurements across Arctic polygonal terrain using LiDAR and NDVI data sets, Water Resour. Res., 50, 6339–6357, doi:10.1002/2013WR014283, 2014.

Gomersall, C. E. and Hinkel, K. M.: Estimating the Variability of Active-La yer Thaw Depth in Two Physiographic Regions of Northern Alaska, Geogr. Anal., 33, 141–155, 2001.

Gross, M. F., Hardisky, M. A., Doolittle, J. A., and Klemas, V.: Relationships among Depth to Frozen Soil, Soil Wetness, and Vegetation Type and Biomass in Tundra near Bethel, Alaska, USA, Arctic Alpine Res., 22, 275–282, 1990.

Harlan, R. and Nixon, J. F.: Geotechnical engineering for cold regions, chap. Ground thermal regime, McGraw-Hill Book Co., New York, N.Y., USA, 103–163, 1978.

Harris, S., French, H., Heginbottom, J., Johnston, G., Ladanyi, B., Sego, D., and van Everdingen, R.: Glossary of Permafrost and Related Ground-Ice Terms, National Research Council of Canada, Ottawa, Technical Memorandum 142, Ottawa, Ontario, Canada K1A 0R6, 1988.

Hinkel, K. M. and Nelson, F. E.: Spatial and temporal patterns of active-layer thickness at Circumpolar Active-Layer Monitoring (CALM) sites in Northern Alaska, 1995–2000, J. Geophys. Res., 108, 667–678, doi:10.1029/2001JD000927, 2003.

Huggett, R. J.: Fundamentals of Geomorphology, Routledge, 2 edn., New York, 2007.

IPCC: Climate Change 2013: The Physical Science Basis. Contribution of Working Group I to the Fifth Assessment Report of the Intergovernmental Panel on Climate Change, Cambridge University Press, Cambridge, UK and New York, NY, USA, doi:10.1017/CBO9781107415324, 2013.

Kane, D. L., Hinzman, L. D., and Zarling, J.: Thermal Response of the Active Layer to Climatic Warming in a Permafrost Environment, Cold Reg. Sci. Technol., 19, 2, doi:10.1016/0165-232X(91)90002-X, 1991.

Kelley, A. M., Epstein, H. E., and Walker, D. A.: Role of vegetation and climate in permafrost active layer depth in arctic tundra of northern Alaska and Canada, J. Glaciol. Climatol., 26, 269–273, 2004.

Khomutov, A. and Leibman, M.: Landslides in Cold Regions in the Context of Climate Change, chap. Assessment of Landslide Hazards in a Typical Tundra of Central Yamal, Russia, Springer International Publishing, 271–290, doi:10.1007/978-3-319-00867-7_20, 2014.

Krieger, G., Moreira, A., Fiedler, H., Hajnsek, I., Werner, M., Younis, M., and Zink, M.: TanDEM-X: A Satellite Formation for High-Resolution SAR Interferometry, IEEE T. Geosci. Remote, 45, 11, doi:10.1109/TGRS.2007.900693, 2007.

Kudryavtsev, V. A., Garagulia, L., Kondratyeva, K. A., and Melamed, V. G.: Fundamentals of Frost Forecasting in Geological Engineering Investigations, Nauka, Moscow. Draft Translation 606, Cold Regions Research And Engineering Lab Hanover N H, 1974.

Lawrence, D. M. and Swenson, S. C.: Permafrost response to increasing Arctic shrub abundance depends on the relative influence of shrubs on local soil cooling versus large-scale climate warming, Environ. Res. Lett., 6, 4, doi:10.1088/1748-9326/6/4/045504, 2011.

Leibmann, M.: CALM SITE R5, https://www2.gwu.edu/~calm/data/webforms/r5_f.html (last access: 8 February 2017), 2016.

Leibman, M., Moskalenko, N., Orekhov, P., Khomutov, A., Gameev, I., Khitun, O., Walker, D., and Epstein, H.: Polar cryosphere of water and land, chap. Interrelation of cryogenic and biotic components of geosystems in cryolithozone of West Siberia on the Transect "Yamal", Paulsen Publisher, Moscow, Russia, 171–192, 2011.

Leibman, M., Khomutov, A., Orekhov, P., Khitun, O., Epstein, H., Frost, G., and Walker, D.: Gradient of seasonal thaw depth along the Yamal transect, in: Proceedings of the tenth international conference on permafrost; translation of Russian contributions, edited by: Melnikov, V., Drozdov, D., and Romanovksy, V., 25–29 June 2012, Salekhard, Yamal-Nenets Autonomous District, Russia, 10, 237–242, 2012.

Leibman, M., Khomutov, A., Gubarkov, A., Mullanurov, D., and Dvornikov, Y.: The research station "Vaskiny Dachi", Central Yamal, West Siberia, Russia – A review of 25 years of permafrost studies, Fennia, 193, 3–30, doi:10.11143/45201, 2015.

Leibman, M. O.: Thaw depth measurements in marine sailne sandy and clayey deposits of Yamal peninsula, Russia: procedure and interpretation of results, in: PERMAFROST – Seventh International Conference (Proceedings), Yellowknife, Canada, 23–27 June 1998, Collection Nordicana, 55, 635–639, 1998.

Leverington, D. W. and Duguay, C. R.: Evaluation of Three Supervised Classifiers in Mapping "Depth to Late-Summer Frozen Ground", Central Yukon Territory, Can. J. Remote Sens., 22, 2, doi:10.1080/07038992.1996.10874650, 1996.

McMichael, C. E., Hope, A. S., Stow, D. A., and Fleming, J. B.: The relation between active layer depth and a spectral vegetation index in arctic tundra landscapes of the North Slope of Alaska, Int. J. Remote Sens., 18, 11, doi:10.1080/014311697217666, 1997.

Melnikov, E. S., Leibman, M. O., Moskalenko, N. G., and Vasiliev, A. A.: Active-Layer Monitoring in the Cryolithozone Of West Siberia, Polar Geography, 28, 267–285, doi:10.1080/789610206, 2004.

Myers-Smith, I. H. and Hik, D. S.: Shrub canopies influence soil temperatures but not nutrient dynamics: An experimental test of tundra snow-shrub interactions, Ecol. Evol., 3, 3683–3700, doi:10.1002/ece3.710, 2013.

Nelson, F. E., Shiklomanov, N. I., Mueller, G. R., Hinkel, K. M., Walker, D. A., and Bockheim, J. G.: Estimating Active-Layer Thickness over a Large Region: Kuparuk River Basin, Alaska, USA, Arctic Alpine Res., 29, 4, doi:10.2307/1551985, 1997.

Pearson, R. G., Phillips, S. J., Loranty, M. M., Beck, P. S. A., Damoulas, T., Knight, S. J., and Goetz, S. J.: Shifts in Arctic vegetation and associated feedbacks under climate change, Nat. Clim. Change, 3, doi:10.1038/nclimate1858, 2013.

Peddle, D. R. and Franklin, S. E.: Classification of permafrost active layer depth from remotely sensed and topographic evidence, Remote Sens. Environ., 44, 1, doi:10.1016/0034-4257(93)90103-5, 1993.

Permafrost Subcommittee, A. C. o. G. R.: Glossary of Permafrost and Related Ground-Ice Terms, Technical Memorandum, National Research Council of Canada, Ottawa, 1988.

Raynolds, M. K. and Walker, D. A.: Increased wetness confounds Landsat-derived NDVI trends in the central Alaska North Slope region, 1985–2011, Environ. Res. Lett., 11, doi:10.1088/1748-9326/11/8/085004, 2016.

Regmi, P., Grosse, G., Jones, M., Jones, B., and Anthony, K.: Characterizing post-drainage succession in thermokarst lake basins on the Seward Peninsula, Alaska with TerraSAR-X backscatter and Landsat-based NDVI Data, Remote Sensing, 4, 3741–3765, doi:10.3390/rs4123741, 2012.

Sazonova, T. S. and Romanovsky, V. E.: A model for regional-scale estimation of temporal and spatial variability of active layer thickness and mean annual ground temperatures, Permafrost Periglac., 14, 125–139, doi:10.1002/ppp.449, 2003.

Schaefer, K., Zhang, T., Bruhwiler, L., and Barrett, A. P.: Amount and timing of permafrost carbon release in response to climate warming, Tellus B, 63, 165–180, doi:10.1111/j.1600-0889.2011.00527.x, 2011.

Schaefer, K., Liu, L., Parsekian, A., Jafarov, E., Chen, A., Zhang, T., Gusmeroli, A., Panda, S., Zebker, H. A., and Schaefer, T.: Remotely Sensed Active Layer Thickness (ReSALT) at Barrow, Alaska Using Interferometric Synthetic Aperture Radar, Remote Sensing, 7, 3735–3759, doi:10.3390/rs70403735, 2015.

Schuur, E. A. G., McGuire, A. D., Schadel, C., Grosse, G., Harden, J. W., Hayes, D. J., Hugelius, G., Koven, C. D., Kuhry, P., Lawrence, D. M., Natali, S. M., Olefeldt, D., Romanovsky, V. E., Schaefer, K., Turetsky, M. R., Treat, C. C., and Vonk, J. E.: Climate change and the permafrost carbon feedback, Nature, 520, 171–179, doi:10.1038/nature14338, 2015.

Shiklomanov, N. I. and Nelson, F. E.: Analytic representation of the active layer thickness field, Kuparuk River Basin, Alaska, Ecol. Model., 123, 2–3, doi:10.1016/S0304-3800(99)00127-1, 1999.

Shiklomanov, N. I., Streletskiy, D. A., Nelson, F. E., Hollister, R. D., Romanovsky, V. E., Tweedie, C. E., Bockheim, J. G., and Brown, J.: Decadal variations of active-layer thickness in moisture-controlled landscapes, Barrow, Alaska, J. Geophys. Res., 115, G00I04, doi:10.1029/2009JG001248, 2010.

Smith, M.: Potential Responses of Permafrost to Climatic Change, J. Cold Reg. Eng., 4, 29–37, 1990.

Ulaby, F. T., Moore, R. K., and Fung, A.: Microwave Remote Sensing – Active and Passive, vol. II, Artech House, Norwood, Mass., USA, 1982.

Ullmann, T., Schmitt, A., Roth, A., Duffe, J., Dech, S., Hubberten, H.-W., and Baumhauer, R.: Land Cover Characterization and Classification of Arctic Tundra Environments by Means of Polarized Synthetic Aperture X- and C-Band Radar (PolSAR) and Landsat 8 Multispectral Imagery – Richards Island, Canada, Remote Sensing, 6, 8565–8593, doi:10.3390/rs6098565, 2014.

Vasiliev, A. A., Leibman, M. O., and Moskalenko, N. G.: Active Layer Monitoring in West Siberia under the CALM II Program, in: Proceedings of the Ninth International Conference on Permafrost, edited by: Kane, D. L. and Hinkel, K. M., 2, 1815–1820, Institute of Northern Engineering, University of Alaska Fairbanks, USA, 28 June–3 July 2008, Fairbanks, Alaska, USA, 2008.

Walker, D., Epstein, H., Leibman, M., Moskalenko, N., Orekhov, P., Kuss, J., Matyshak, G., Kaarlejärvi, E., Forbes, B., Barbour, E., and Gobroski, K.: Data Report of the 2007 and 2008 Yamal Expeditions, Alaska Geobotany Center, Institute of Arctic Biology, University of Alaska Fairbanks, Fairbanks, AK, USA, 121 pp., 2009.

Wang, C., Zhang, H., Wu, Q., Zhang, Z., and Xie, L.: Monitoring permafrost soil moisture with multi-temporal TERRASAR-X data in northern tibet, Geoscience and Remote Sensing Symposium (IGARSS), 2016 IEEE International, 10–15 July 2016, Beijing, China, doi:10.1109/IGARSS.2016.7730558, 2016.

Werninghaus, R., Balzer, W., Buckreuss, S., Mittermayer, J., and Mühlbauer, P.: The TerraSAR-X Mission, in: SPIE 5236, SAR Image Analysis, Modeling, and Techniques VI, doi:10.1117/12.511500, 2004.

Wessel, B.: TanDEM-X Ground Segment – DEM Products Specification Document, Projektbericht, EOC, DLR, Oberpfaffenhofen, Germany, Public Document TD-GS-PS-0021, Issue 3.0., 2013.

Widhalm, B., Bartsch, A., Siewert, M. B., Hugelius, G., Elberling, B., Leibman, M., Dvornikov, Y., and Khomutov, A.: Site scale wetness classification of tundra regions with C-band SAR satellite data, in: Proc. "Living Planet Symposium 2016", Prague, Czech Republic, ESA SP-740, 9–13 May 2016.

Yershov, E. D.: General Geocryology, Cambridge University Press, Cambridge, UK, 1998.

Zhang, Z., Wang, C., Tang, Y., and Zhang, H.: Surface deformation monitoring using time series TerraSAR-X images over permafrost of Qinghai-Tibet Plateau, China, Geoscience and Remote Sensing Symposium (IGARSS), 2016 IEEE International, 10–15 July 2016, Beijing, China, doi:10.1109/IGARSS.2016.7730558, 2016.

Zwieback, S., Liu, X., Antonova, S., Heim, B., Bartsch, A., Boike, J., and Hajnsek, I.: A Statistical Test of Phase Closure to Detect Influences on DInSAR Deformation Estimates Besides Displacements and Decorrelation Noise: Two Case Studies in High-Latitude Regions, IEEE T. Geosci. Remote, 54, 5588–5601, doi:10.1109/TGRS.2016.2569435, 2016